IET Electric Power Applications

Research Article

IET Journals
The Institution of Engineering and Technology

Design of a wind turbine generator for rural applications

ISSN 1751-8660
Received on 26th October 2018
Revised 27th December 2018
Accepted on 21st January 2019
E-First on 27th February 2019
doi: 10.1049/iet-epa.2018.5734
www.ietdl.org

Cristian Ruschetti[1], Carlos Verucchi[1] ✉, Guillermo Bossio[2], Guillermo García[2], Matias Meira[1]

[1]*UNCPBA, INTELYMEC - CIFICEN (UNCPBA, CICPBA, CONICET), Del Valle 5737, Olavarría, Argentina*

[2]*UNRC, GEA, Argentina*

✉ *E-mail: verucchi@fio.unicen.edu.ar*

Abstract: This paper presents a wind-generation system design for rural applications. In Southern areas of Argentina, there are right conditions for wind energy exploitation. Depending on the characteristics of these areas, the wind-generation systems can operate either isolated or connected to the grid. This work particularly emphasises the design of a generator to optimise the system performance and achieve its minimum volume. The analytical design is evaluated using finite element analysis and experimentally validated using a 35 kW prototype. The tests reveal that the design procedure is suitable. The initially proposed efficiency aim was exceeded, reaching a maximum value of 94.2%. The generator operating conditions make it particularly suited for the application for which it was designed.

1 Introduction

Numerous studies have revealed that Patagonia, a region located at the southern end of Argentina, is a suitable area for the exploitation of wind resources [1]. In [2] are presented annual wind speed variations for this area. The average speed is 7.7 m/s with a 40% probability of occurrence. These values are above the minimum one required to guarantee the viability of power companies to produce electric energy. Although these areas are far from major consumption centres, it is possible to connect wind power generators to the grid or, as proposed in [3], to combine wind and other energy sources to reduce CO2 emissions. There is another possibility to exploit wind resources in the region through isolated small plants. This is the alternative presented in this work. That is, from the characteristics of the region (very low population density, large number of small rural settlements and low annual rainfall), it arises the necessity of using generation systems able to supply energy to both small isolated consumption areas and those grouped in wind farms, while supplying energy to the power grid.

It can be concluded that the region under analysis presents suitable characteristics for the installation of low-power wind turbines able to:

(a) Feed small isolated plants through diesel-wind hybrid systems of up to 100 kW.
(b) Feed water pumping systems for irrigation.
(c) Provide a system for the 'self-powered' market. That is, for individuals to supply their own consumption and supply the exceeding energy to the power grid.
(d) Regulate voltage on weak lines, especially in rural areas.
(e) Facilitate the interconnection of small- and medium-sized power systems, both direct current (DC) and alternating current (AC) systems, such as plants and hydrogen fuel cells or photovoltaic cells, and three-phase generators of primary energy sources, as for instance diesel, hydro, or gas, respectively.

In [2], it is presented a comprehensive study on the possibilities to generate wind energy in Patagonia. This study proposes a methodology to find the most suitable areas for energy exploitation. In [4], it is presented the design of low-power wind generators for rural purposes and compares the different design possibilities depending on the characteristics of the turbine.

In addition, it is important to notice that the systems used to generate electricity from wind power are generally composed of a three-blade horizontal axis turbine plus an electric generator. A wind turbine is designed to produce power over a range of wind speeds. The cut-in speed is around 3–4 m/s for most turbines, and it operates up to a rated speed of 12 to 15 m/s with a fixed step. If the rated wind speed is exceeded, the power has to be limited and one way to achieve this is by using the blade pitch control. In order to protect the mechanical system, the speed cut-out is around at 25 m/s [5].

The optimum operation speed values of wind turbines are below those of electric generators such as doubly fed induction machines. This requires the use of gear boxes as speed multipliers between the turbines and generators. These gear boxes increase the system costs, producing in addition a decrease in its overall performance. They also require more maintenance due to they are the major cause of failure in wind turbines, producing also unwanted noise [6, 7].

Since the nineties, designers have proposed some generators directly coupled to the wind turbines [8, 9], for which it is necessary to build low-speed generators with a high number of magnetic poles.

An alternative to build low-speed generators is the use of permanent magnet electrical machines with rare earth magnets of high energy, such as NdFeB alloys (Neodymium -Iron-Boron). A reduction of volume and weight of the generators and its improvements in their performance are some of the advantages of using permanent magnet synchronous machines (PMSM).

Most PMSMs use surface-mounted magnets in an inner rotor [6]. Chen *et al.*, on the other hand, proposes the use of axial-flow geometries of permanent magnet (PM) assembly, which are appropriate for high number of poles [10]. Another alternative is proposed by Olano [11] and Choi *et al.* [12], which consists in mounted PMs on an outer rotor. This installation can be simplified by coupling the turbine blades directly to the outer rotor.

Regarding the type of windings used to build the generator, there are several possible alternatives. A general classification of stator windings for PMSM distinguishes between distributed and concentrated windings. The concentrated windings can be subdivided into double-layered overlapped and single-layered non-overlapped. Concentrated windings presents advantages over distributed ones since they offer a reduction in copper volume and losses due to Joule effects, as well as improvements in performance and an increase in power density [13].

Finally, it is necessary to note that a phenomenon known as 'cogging torque' is common in PMSM. Such phenomenon is the

product of the magnetic interaction between the rotor poles and the stator teeth. The number of equilibrium positions of the rotor is defined as the least common multiple between the number of slots and the number of poles. Though the average value of reluctance torque is zero, its presence can result in high starting torques and levels of vibration, for which it is recommended to reduce the cogging torque. Different solutions have been proposed that either modify the profile of PMs or fractionate them into longitudinal sections to reduce this effect [14].

This work aims to present the general characteristics of the proposed installation and specifically the permanent-magnet synchronous generator (PMSG) design. In the following sections of this paper, the general characteristics of the proposed installation are presented as well as the design of the generator. A verification using finite elements analysis (FEA) is carried out. Finally, experimental results from a build prototype are obtained.

2 General installation characteristics

The power characteristic of the direct drive wind turbine developed is presented in Fig. 1. For this particular case, speed values are within the range 6 to 12 m/s without pitch control. Above 12 m/s, the blades are re-oriented in order to keep a constant speed with the turbine rotating at about 150 rpm. If speed values exceed 25 m/s, the blades orientate so that the turbine stops rotating and turns off. All these speed values are defined based on the wind characteristics in Patagonia areas. For this operation mode, the generator output voltages vary directly with the turbine rotation speed. The frequencies of the generated voltages are also variable depending on speed variations. To achieve a three-phase output system with constant voltage and frequency, an electronic converter is generally used. It rectifies the generator output voltage and then generates a useful AC frequency. In this application, Argentina grid-rated values are adopted (380 V and 50 Hz).

A scheme of the proposed installation is presented in Fig. 2. The energy produced by the generator is rectified and then converted into AC at the grid frequency. The DC bus allows energy storage in a battery bank. An additional option offers the possibility of including a conventional generator powered by a diesel engine. The maximum output power is fixed at 32 kW. Thus, the generator is designed for a nominal power of 35 kW.

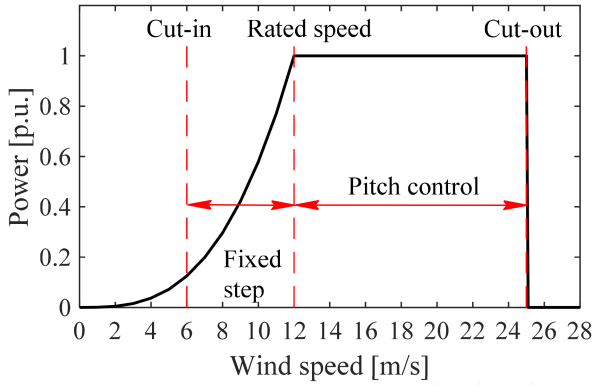

Fig. 1 *Power curve of the wind turbine developed*

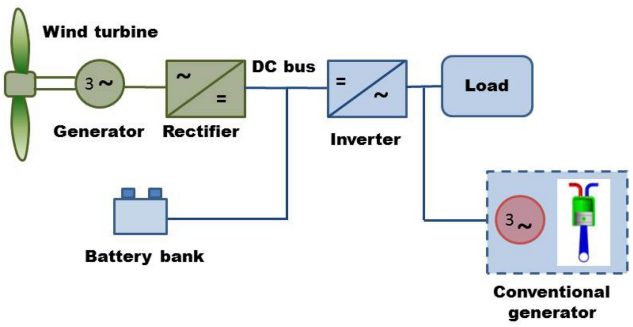

Fig. 2 *Installation Scheme*

As shown in [8], there is an optimal ratio between the tangential speed of the tip of a blade and the actual speed of the wind defined as 'tip speed ratio':

$$\lambda = \frac{r\omega_r}{v} \tag{1}$$

where ω_r is the angular speed of the turbine, r is the radius of the blades and v, the wind speed. To reach optimal power coefficients in three-bladed turbines, it is necessary to achieve a value of $\lambda = 7$, then, with a wind speed of 12 m/s it is adopted a rotation speed of 150 rpm (as suggested in [8] for power of 35 kW). Then, $r = 5.3$ m.

3 Generator design

3.1 General dimensions

The design of an electrical machine is an iterative process. This section presents the procedure to obtain the initial dimensions of the geometry and the windings. These dimensions are calculated using software that combines analytical calculation and heuristics procedures. Then, they are verified using FEA.

Outer rotor topology was adopted due to the advantages it offers in the construction and assembly of the generator [6]. Regarding the stator windings, double-layer fractional pitch windings are used in order to reduce cogging torque and copper losses.

To select the number of poles and generator slots, it becomes necessary to define the most suitable option with respect to the number of slots per pole and per phase (q) [15]:

$$q = \frac{Q}{mp} \tag{2}$$

where Q is the number of stator slots, m is the number of phases and p the number of poles of the generator.

Values of $q < 1$ determine fractional pitch windings. This feature makes the coil heads shorter and allows reducing copper losses. For this particular design, it is proposed a value of q so as to obtain an electromotive force (EMF) with low harmonic distortion and therefore a waveform close to a sinusoidal one. A topology is proposed in which the fundamental winding factor k_1 is close to 1. Finally, the possibility of limiting the cogging torque through the choice of q is discussed. Therefore, and based in [16], a value of $q = 0.75$ is adopted.

The relationship between rotation speed and frequency, in a synchronous machine, is given by:

$$n = \frac{120f}{p} \tag{3}$$

where f is the frequency of the induced voltages. In order to obtain a frequency near 50 Hz, it is chosen $p = 36$. Then, according to (2), $Q = 81$.

According to [15], the dimensions of the machine air gap are directly dependant on,

$$S_{\text{nom}} = \eta \frac{\sqrt{2}\pi^2 n}{120} k_1 f_a D_{os}^2 l_s \widehat{B}_{g1} K_s \tag{4}$$

where S_{nom} is the nominal apparent power of the generator, η represents the efficiency, factor k_1 is the stator winding factor, f_a is the stacked plates, D_{os} is the stator outer diameter, l_s, the length of the plate stacking, B_{g1} is the amplitude of the fundamental component of flux density in the air gap and K_s is the linear density of current on the air-gap perimeter in A/m.

In [15], there are suggested optimum values for the relationship between the stator outer diameter and the air gap length. For the proposed number of poles, the ratio is 2.5. Thus, from (4), it can be obtained the following dimensions: $D_{os} = 683$ mm and $l_s = 149$ mm.

Then, it is possible to obtain the slot pitch from the stator outer diameter as,

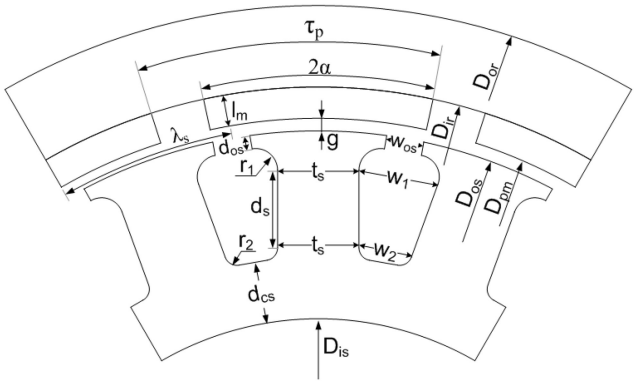

Fig. 3 *Generator topology and general dimensions*

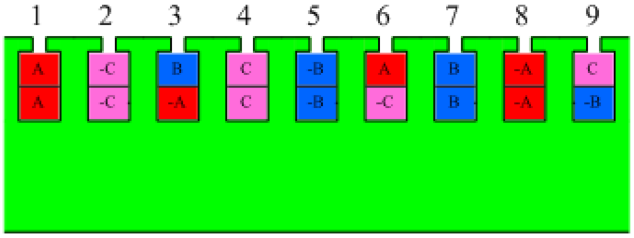

Fig. 4 *Scheme of the winding, 81slots, 36 poles*

$$\lambda_s = \frac{D_{os}}{Q} = 26.48\,\text{mm} \tag{5}$$

In [17], it is proposed dividing the slot pitch into equal parts to obtain the tooth and slot widths (w_1 and t_s in Fig. 3).

The PMs are arranged on the rotor inner surface, as illustrated in Fig. 3. If the PMs occupy an arc of 2α electrical degrees, then the maximum induction in the air gap may be calculated according to [18], as:

$$\hat{B}_{g1} = \frac{4}{\pi} B_{g0}(\alpha) \tag{6}$$

where B_{g0} is the average induction in the air gap.

The maximum value of B_{g1} is 1.1 T, determined depending on the silicon saturation of the steel plates. The angle α is chosen equal to 60 electrical degrees, as recommended in [18], who demonstrates that around this value, there is an optimum point in term of cost. The mean value of flux density in the air gap (B_{g0}) is 0.998 T. Given B_{g0}, and choosing the tooth width t_s equal to the slot width w_1, then, the maximum tooth density becomes 1.995 T.

3.2 Permanent magnets design

In order to optimise the machine performance through its design, it is proposed the use of NdFeB PMs, whose residual flux density is around 1.2 T. Its energy product is 300 kJ/m^3 and can reach a safe operation temperature up to 150°C [19].

Based on Ampere's law, on a basic magnetic circuit, without magnetomotive force (MMF) and where the PM establishes the magnetic flux

$$F_{\text{MM}} = H_m l_m + H_{g0}\, g = 0 \tag{7}$$

where g is the air gap thickness, H_m is the PM magnetic field, l_m is the PM height y H_{g0} is the air gap magnetic field. Furthermore, if the cross-sections of the permanent magnets and air gap are equal to

$$B_m = B_{g0} \tag{8}$$

where B_m is the PM induction. Taking into account the B_m–H_m linear characteristic of the NdFeB, in the working point of the PM [18] and knowing that the relative permeability of the material is ~1

$$B_m = \mu_0 H_m + B_r \tag{9}$$

where B_r is the PM residual flux density (1.2 T for NdFeB). Getting H_m from (9), replacing it in (7) and considering the air gap permeance irregularity through the Carter coefficient,(C_c) the relation between the intended B_{g0} and the PM residual induction is given by,

$$B_{g0} = \frac{l_m}{l_{ge}} B_r \tag{10}$$

where l_{ge} is the gap effective length, given by,

$$l_{ge} = (l_m + g) C_c \tag{11}$$

Given that PM permeability in the direction of its magnetisation is practically equal to that of air, its height is added to that of the gap, as shown in (11). Moreover, considering that the air gap of the machine is modified by the stator slots, its length must be corrected using the Carter coefficient, whose value is chosen based in [18].

Thus, taking a $g = 1.5$ mm, $C_c = 1.05$ and $B_r = 1.2$ T, yields $l_m = 10.3$ mm.

3.3 Core design

The core design consists of calculating the height of the circuit components for which the magnetic flux of stator and rotor closes. This is commonly called 'yoke' and requires knowing the flux per pole of the machine [18]:

$$\varphi_p = \frac{2}{\pi} \hat{B}_{g1} \frac{\pi D_{os}}{p} l_s = 0.0062 Wb \tag{12}$$

The thickness of the stator core is dimensioned so that the flux density B_{cs} does not exceed 1 T. This density value is calculated as,

$$B_{cs} = \frac{\varphi_p}{2} \frac{1}{d_{cs} f_a l_s} \tag{13}$$

Then, the yoke height d_{cs} must be 21.29 mm.

Slots are sized considering its width (w_1) and the tooth thickness (t_s) equal. The depth of slots d_s, as a first approximation, is chosen equal to five times the width w_1.

3.4 Winding design

It is adopted a double-layered overlapped winding. Since the winding considers a fractional value q, the coils of each phase should be located according to the diagram of Fig. 4. The beginnings and endings of coils for each phase are represented by A, B, and C and by −A, −B and −C, respectively. The winding step (y) is equal to 2. Fig. 4 only shows nine slots because this pattern repeats for the remaining stator slots.

To calculate the number of turns per coil and the wire diameter, it should be noted that the induced EMF at each phase, for a double-layered overlapped winding with all the coils in series, is given, according to [5], by:

$$E_s = 4.44 f k_1 q p N_b \varphi_p \tag{14}$$

where, N_b is the number of turns per coil. Given that the voltage drops at each phase cannot be known, and considering a desirable voltage at the terminals of 220 V per phase at nominal rate, it is initially assumed a no load voltage of 250 V. Therefore, the turns per coil result $N_b = 8$.

Finally, the maximum wire diameter is calculated assuming a slot usage factor ($f_{ar} = 0.4$).

Table 1 General dimensions of the designed machine

Parameter	Analytical res.	RMxprt res
D_{os}	682.85 mm	700 mm
l_s	148.97 mm	150 mm
K_s	30 kA/m	28.353 kA/m
λ_s	26.48 mm	27.15 mm
g	1.5 mm	1.6 mm
l_m	10.30 mm	12 mm
d_m	39.73 mm	40 mm
l_{pm}	49.66 mm	50 mm
r_1	5 mm	6.33 mm
r_2	5 mm	3.62 mm
d_{os}	3 mm	3 mm
w_{os}	4 mm	5 mm
t_s	12.93 mm	13.8 mm
w_1	12.93 mm	12.66 mm
d_s	64.66 mm	70 mm
w_2	7.92 mm	7.24 mm
D_{is}	484.95 mm	480 mm
D_{pm}	685.85 mm	703.2 mm
D_{ir}	706.45 mm	727.2 mm
D_{or}	749.03 mm	766 mm
N_b	8	8
d_{cu}	2.3 mm	2.3 mm

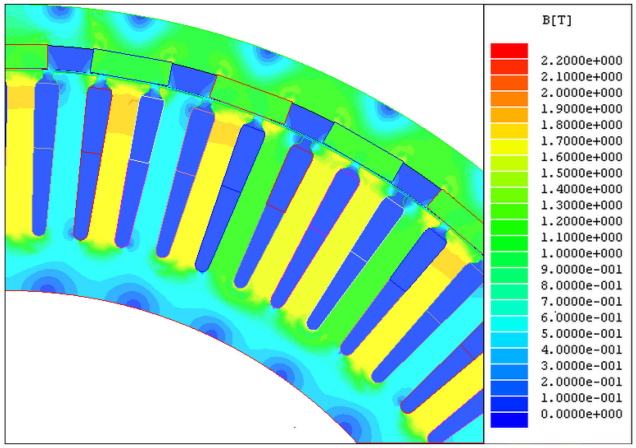

Fig. 5 *Magnetic Induction obtained through FEA*

$$d_{cu} = \sqrt{\frac{f_{ar} d_s}{\pi N_b}(w_1 + w_2)} \tag{15}$$

3.5 Design optimisation

With all the preliminary dimensions so far obtained, it begins an iteration process with the purpose of adjusting these dimensions in order to reduce the generator volume while maintaining its efficiency above 92%. This efficiency value is determined based on typical values for this type of machines [15]. The optimisation process is carried out using the methodology proposed in [20]. The variables adjusted during the optimisation process are the rotor diameter, some slots dimensions, and the PMs length and height. The optimisation process was carried out maximising the efficiency and looking for keep bounded the structure weight. For this, the slot filling percentage is increased to reduce electrical losses. Moreover, avoiding magnetic induction concentration areas, the magnetic losses are limited. The dimensions adopted are shown in Table 1.

Finally, the stator resistance and inductance can be calculated as well as voltage drops, losses, efficiency, cogging torque, and PM demagnetisation. The verification of all these values can be seen in [21].

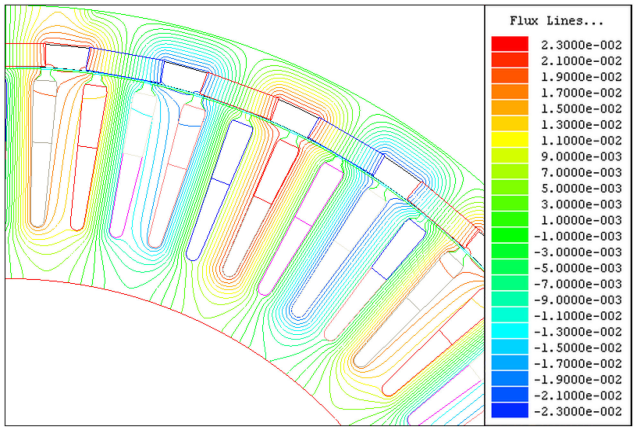

Fig. 6 *Magnetic field distribution on the generator*

Fig. 7 *Generator mounted on test bench*

4 FEA verification

For the FEA, bi-dimensional software is used since radial-flux laminated-stator machines allow obtaining satisfactory results avoiding high computational costs. As a first step, a magneto-static analysis is carried out with the objective of verifying the border conditions and the magnetisation direction of PMs.

This software automatically generates the global equation system, which can be solved using either the Incomplete Cholesky Conjugate Gradient (ICCG) method or the direct elimination method for linear equations. Fig. 5 presents values for magnetic induction for a sector of the generator. These values are obtained through the FEA and match those of the analytical design with minor differences, no more than 3%. Fig. 6 presents the distribution of magnetic flux without load.

Likewise, losses and machine performance are also verified, as well as internal voltage drops and cogging torque, showing that the obtained results practically match those estimated in the analytical design [21].

5 Experimental verification

A prototype was built to experimentally validate the proposed design. It can be observed in Fig. 7 the generator mounted on a testing bench that consists of a speed reducer and an induction motor used to drive the generator. The test bench also includes resistive loads. With it is application and using a load cell it is possible to measure the induced torque of the generator.

Different tests were carried out on the generator to validate the proposed design. No-load tests show values for voltage drops of ~440 V. These values show differences <1% compared to those predicted using the FEA. The voltage harmonics are about 1% the fundamental component for the 5th harmonic and 0.2% the fundamental component for the 7th harmonic. This determines a THD = 1.2%.

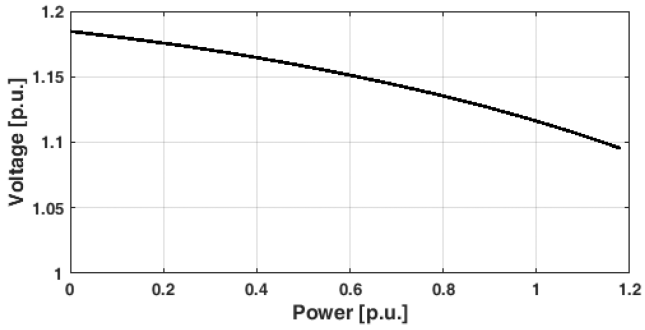

Fig. 8 *Voltage at the terminals vs. output power*

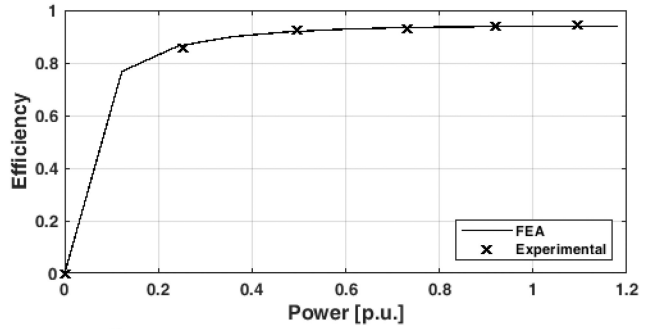

Fig. 9 *Efficiency vs. output power*

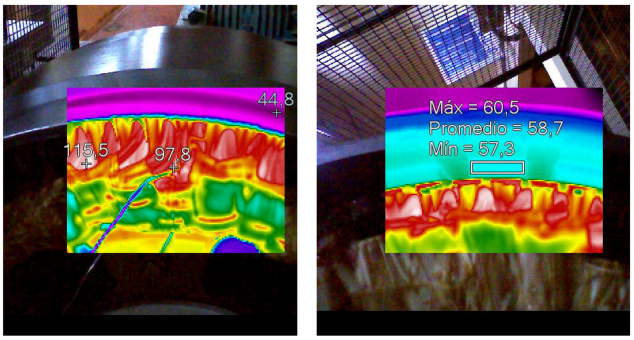

a *b*

Fig. 10 *Temperature reached by the generator components*
(a) Windings, ***(b)*** Permanent magnets

Fig. 8 presents voltage regulation at the generator terminals for variations of load between no-load condition and 120% of nominal load. The voltage regulation for nominal load with unity power factor is ∼5%. During the design process, no restrictions are imposed on internal voltage drops, focusing on the machine performance. Given that the generator output voltages are rectified, voltage drops are acceptable.

Results for the generator under load conditions are shown in Table 2. Stepwise loads were applied up to the nominal value. The generator efficiency, at rated speed, is 94%, higher than the estimated one. This value is comparable to the results for a 30 kW rated power and 48 poles PMSG presented in [22]. The generator efficiency for different loads with unity power factor can be observed in Fig. 9. The mean absolute percentage error (MAPE) between the experimental and the FEA results is 0.45%. This is a very acceptable value taking into account that in FEA model, the magnetic losses were carried out through a function. The function coefficients were obtained for the whole induction working range of the core material. Furthermore, the friction losses were estimated from typical values.

The increase of temperature for nominal load is 80°C. Fig. 10 presents a thermal infrared image that corresponds to one of the tests. It is important to notice that tests were carried out under disadvantageous cooling conditions, in complete absence of ventilation. Under normal operation conditions, and taking advantage of wind refrigeration, the temperature jumping results always lower than that estimated ones.

Table 2 Experimental results

Variable	LOAD				
	6 [kW]	12 [kW]	18 [kW]	24 [kW]	30 [kW]
input torque [Nm]	607.70	1106.76	1612.36	2047.72	2447.95
input power [kW]	9.68	17.62	25.66	32.62	38.96
output power [kW]	8.30	16.30	23.95	30.71	36.70
η (%)	85.7	92.5	93.3	94.2	94.2
$\cos(\varphi)_{Load}$	1	1	1	1	1
phase current [A]	10.88	21.69	31.90	41.74	51.10
unbalance I [%]	2.62	2.23	1.02	0.96	1.01
THD I [%]	1.86	1.73	1.63	1.61	1.53
line voltage [V]	453.75	447.74	439.82	431.67	421.63
unbalance V [%]	0.72	0.73	0.84	0.86	0.87
THD V [%]	1.36	1.48	1.56	1.53	1.45
f [Hz]	45.64	45.63	45.60	45.64	45.60

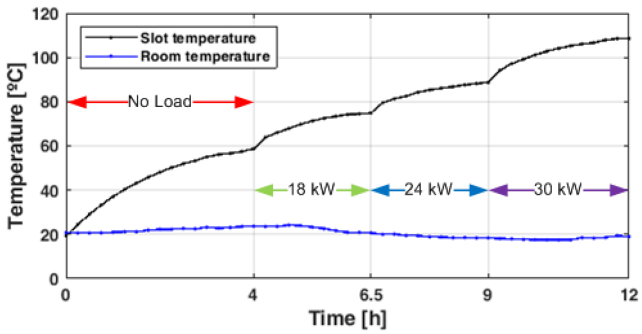

Fig. 11 *Evolution of temperature inside the slots*

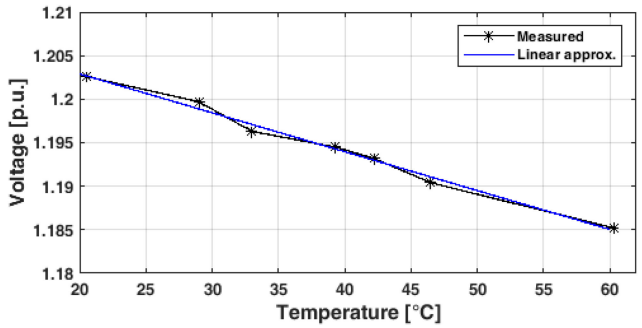

Fig. 12 *Reduction of the induced EMF due to temperature effects*

Fig. 11 shows the temperature evolution inside a slot in the upper part of the generator for different load values. It is important to verify the temperature inside the magnets since if it exceeds certain values, then residual magnetism losses will occur and they will be irreversible. In [23, 24], residual magnetism losses at any generator pole is deeply analysed and techniques of easy implementation for faults detection due to loss of magnetism are proposed. Fig. 12 presents the induced EMF variation due to temperature. The experimental result is approximate with a linear least squares fitting, with an acceptably low level of root mean square error (RMSE) of 5.26×10^{-4} and a coefficient of determination $R^2 = 0.9904$. Therefore, the linear fitting correctly represents the analysed characteristic. Knowing the temperature effect over the EMF allows predicting its reduction under operation conditions. The linear approximation gives a 0.045% FEM reduction rate, while the B_r reduction rate for the NdFeB PM used in this prototype is three times higher. The difference between the reduction rates is due to the magnetic core saturation. This characteristic results advantageous for voltage regulation.

6 Conclusions

A proposal for the exploitation of wind energy in areas with particular characteristics was presented. This proposal consists in designing and building installations that aim to meet small and medium loads demands, provide energy for artificial irrigation, supply the exceeding energy to the power grid, and compensate voltage drops in lines. The electric generator was designed to work directly coupled to the turbine. It consists of a PM outer rotor and fractional pitch windings. A geometry optimisation was carried out by analysing the analytical design using FEA, with the objective of maximising the machine efficiency and reducing its volume. The experimental tests allow concluding that the design procedure is suitable. Understanding that the procedure combines analytical and FEA design, it was reached a 94.2% generator efficiency, with a 0.45% MAPE respect off the numerical model. This high efficiency and the generator operating conditions make it particularly suited for the application for which it was designed.

This proposal is an alternative to conventional methods to produce and take advantage of wind energy in rural areas of low population.

7 Acknowledgments

This research was supported by the ANPCYT, CONICET, Universidad Nacional del Centro de la Provincia de Buenos Aires and Universidad Nacional de Río Cuarto (Argentina).

8 References

[1] Lássig, J., Cogliati, M., Bastanski, M., *et al.*: 'Wind characteristics in neuqen, north Patagonia, Argentina', *Wind Eng. Ind. Aerodyn.*, 1999, **79**, pp. 183–199

[2] Oliva, R.: 'Simulation and measurement for effective isolated wind hybrid system development in south Patagonia', *Energy. Sustain. Dev.*, 2008, **12**, (2), pp. 17–26

[3] Spazzafumo, G.: 'South Patagonia: wind/hydrogen/coal system with reduced CO_2 emissions', *Hydrog. Energy*, 2013, **38**, pp. 7599–7604

[4] Al-Bahadly, I.: 'Building a wind turbine for rural home', *Energy. Sustain. Dev.*, 2009, **13**, (3), pp. 159–165

[5] Gönen, T.: '*Electrical machines with MATLAB*' (CRC Press, United States, 2012, 2nd edn.)

[6] Ki-Chan, K., Seung-Bin, L., Ki-Bong, J., *et al.*: 'Analysis on the direct-driven high power permanent magnet generator for wind turbine'. Proc. Eighth Int. Conf. on Electrical Machines and Systems, Nanjing, China, 2006, pp. 243–247

[7] Fengxiang, W., Jianlong, B., Qingming, H., *et al.*: 'Design features of low speed permanent magnet generator direct driven by wind turbine'. Proc. Eighth Int. Conf. on Electrical Machines and Systems, Nanjing, China, 2006, pp. 1017–1020

[8] Chen, J., Nayar, C., Xu, L.: ' design and finite-element analysis of an outer-rotor permanent-magnet generator for directly coupled wind turbines', *IEEE Trans. Magn.*, 2000, **36**, (5), pp. 3802–3809

[9] Khan, M., Pillay, P., Malengret, M.: 'Impact of direct-drive WEC systems on the design of a small PM wind generator'. Proc. IEEE Power Tech. Conf., Bologna, Italia, 2003, pp. 7–13

[10] Chen, Y., Pillay, P.: 'Axial-flux PM wind generator with a soft magnetic composite core'. Proc. Industry Applications Conf., Hong Kong, China, 2005, pp. 231–237

[11] Olano, A., Moreno, V., Molina, J., *et al.*: 'Design and construction of an outer-rotor PM synchronous generator for small wind turbines; comparing real results with those of FE model'. Proc. Electrical Machines, ICEM, Sydney, Australia, 2008, pp. 1–6

[12] Choi, J., Jang, S.-M, Song, B.-M.: 'Design of a direct-coupled radial-flux permanent magnet generator for wind turbines'. IEEE Power and Energy Society General Meeting, Minnesota, USA, 2010, pp. 1–6

[13] El-Refaie, A.: 'Fractional-slot concentrated-windings synchronous permanent magnet machines: opportunities and challenges', *IEEE Trans. Ind. Electron.*, 2010, **57**, (1), pp. 107–121

[14] Islam, R., Husain, I., Fardoun, A., *et al.*: 'Permanent-magnet synchronous motor magnet designs with skewing for torque ripple and cogging torque reduction', *IEEE Trans. Ind. Appl.*, 2009, **45**, (1), pp. 152–160

[15] Lipo, T.: '*Introduction to AC machine design*' (Wiley IEEE Press, United States, 2017)

[16] Hanselman, D.: '*Brushless permanent magnet motor design*' (Electrical and Computer Engineering University of Maine, USA, 2006)

[17] Pyrhönen, J., Jokinen, T., Hrabovcová, V.: '*Design of rotating electrical machines*' (John Wiley & Sons Ltd., Great Britain, 2009)

[18] Slemon, G.: 'On the design of high-performance surface-mounted PM motors', *IEEE Trans. Ind. Appl.*, 1994, **30**, (1), pp. 134–140

[19] Sebastian, T.: 'Temperature effects on torque production and efficiency of PM motors using NdFeB magnets', *IEEE Proc. Ind. Appl.*, 1995, **31**, (2), pp. 353–357

[20] He, Q., Wang, Q.: 'Optimal design of low-speed permanent magnet generator for wind turbine application'. Proc. Power and Energy Engineering Conf., Shanghai, China, 2012, pp. 1–3

[21] Ruschetti, C.: 'Diseño de generadores sincrónicos de imanes permanentes de velocidad variable para turbinas eólicas', Phd. Thesis, Universidad Nacional de Río Cuarto Press, 2012

[22] Bazzo, T., Kolzer, J.F., Carlson, R., *et al.*: 'Optimum design of a high-efficiency direct-drive PMSG'. 2015 IEEE Energy Conversion Congress and Exposition (ECCE), Montreal, QC, 2015, pp. 1856–1863

[23] Ruschetti, C., Bossio, G., De Angelo, C., *et al.*: 'Effects of partial rotor demagnetization on permanent magnet synchronous machines'. Proc. IEEE Int. Conf. on Industrial Technology, Viña del Mar, Chile, 2010, pp. 1233–1238

[24] Ruschetti, R., Verucchi, C., Bossio, G., *et al.*: 'Rotor demagnetization effects on permanent magnet synchronous machines', *Energy Convers. Manage.*, 2013, **74**, pp. 1–8